

A principled approach to biological motor control for generating humanoid robot reaching movements

Tran Minh Tuan, Philippe Souères, Michel Taïx and Emmanuel Guigon

Abstract—This paper presents an application of neurobiological motor principles to the control of humanoid robot reaching movements. The model is mainly based on the hypotheses that the energy of motoneurons signals is continuously minimized along the motion and that dynamic and static efforts are processed separately. This paradigm is used to control the robot HRP2 by considering a dynamic model of the arm including, for each degree of freedom, two second order low-pass filters modeling the neuromuscular system defined by a pair of antagonist muscles. The optimal control problem is solved as a nonlinear programming problem by using a direct transcription method coupled with the optimization software Ipopt. This approach allows to generate realistic movements with anthropomorphic features such as quasi-rectilinear trajectories and bell-shaped velocity.

Keywords: human motor control, neurobiological principles, reaching control, humanoid robot, direct transcription, nonlinear programming.

I. INTRODUCTION

Even though humanoid robots strongly differ from humans in their mechanical structure, their sensing and actuation capabilities, and the way of processing data, the knowledge of neurobiological motor principle turns out to be of great interest to reduce the complexity of the control problem and provide robots with anthropomorphic motor capabilities.

We focus here on the control of reaching movements. For this problem, different kinds of biologically inspired approaches have so far been proposed in robotics. Some authors made a special effort to reproduce the mechanical musculoskeletal structure of the human arm and develop control strategies involving the dynamics of internal forces [1], or replicate biological patterns of muscle activity [2]. Other authors tried to characterize trajectories by minimizing of a particular cost function such as variance [3], torque [4], jerk [5], or energy. Several control architectures were also proposed to reproduce the multi-referenced brain processing and its plasticity [6]. Finally, motion capture techniques were used by numerous authors to execute human-like motions [7], [8]. However, beyond imitation, the application of biological motor principles seems to be a way to produce canonical movements in any situation.

T. Minh and P. Souères are with LAAS-CNRS, University of Toulouse, 7 avenue du Colonel Roche, F-31077 Toulouse, France

M. Taïx is with University of Toulouse, University Paul Sabatier, 118 Route de Narbonne, F-31062 Toulouse, France {tmtuan, soueres, taix}@laas.fr

E. Guigon is with INSERM U742, ANIM, UPMC, University of Paris 06, 9 quai Saint-Bernard, F-75005 Paris, France guigon@ccr.jussieu.fr

This paper presents an application of a recent biologically inspired computational theory based on a principled approach to motor control [9], [10]. This theory, which can accurately account for kinematics, kinetics, muscular, neural, and stochastic characteristics of redundant reaching movements, is applied here to the control of the humanoid robot HRP2. The approach is grounded on the idea that the central nervous system (CNS) processes dynamic efforts (inertial, velocity dependent) and static efforts (elastic, gravitational) separately, and that the energy of motoneurons is continuously minimized during motion. In order to apply these principles to the control of HRP2, a global model is considered, which contains the dynamics of the six degrees-of-freedom (DOF) robot arm and includes, for each DOF, an additional filter simulating the dynamics of a pair of virtual antagonist muscles. As a result, it will be shown that the robot arm movements obtained with this approach exhibit the main features of human motions, namely: quasi rectilinear hand trajectories and bell-shaped single peak velocity profiles.

The paper is organized as follows. The neurobiological motor principles which are at the basis of our work are summarized in section II. The global model and the problem statement are presented in section III. Section IV deals with the characterization of minimum-energy trajectories satisfying the boundary conditions. Finally, simulation results are presented in section V.

II. THE BIOLOGICAL PRINCIPLES OF MOTOR CONTROL

Breakthroughs into the understanding of motor functions have generally been brought about by computational studies that disclose functioning principles independent of brain structures or neural processes. The model proposed by Guigon et al. [9], [10] provides a unified account of motor behavior by making the hypothesis that motor control is mainly governed by the following four principles.

Separation principle: There is a substantial experimental evidence to support the idea that static and dynamics forces are processed separately by the CNS. Psychophysical studies have shown that velocity profiles remain unchanged when moving in a known constant or elastic force field, but that they are in general modified by time and amplitude scaling in velocity-dependent and inertial fields [11]. EMG studies have revealed additive velocity-independent, tonic and velocity-dependent, phasic components which have been related to the generation of anti-gravity torques and dynamic torques,

respectively [12]. A similar additive combination between tonic and phasic activity was observed in neurons of primate motor cortex [13]. Finally, experiments have shown that the terminal posture of 3D redundant movements is independent of velocity [14]. As the relative contribution of anti-gravity and dynamic torques varies with velocity, optimization of the total torque pattern would predict variations of terminal posture with velocity. This result suggests that dynamic forces are optimized independently of static forces.

Optimal feedback control principle: The CNS processes an optimal control of dynamic forces that is appropriate for an online regulation of movements. Though optimal control has been repeatedly used to account for many aspects of motor control, e.g. trajectory formation, muscular redundancy, postural control, locomotion, etc. [15], [16], [17], it has rarely been applied to the case of nonlinear redundant systems [18]. The difficulty is to account for the simultaneous control of posture and movement. Most studies did not consider the case of static forces due to the difficulties to solve optimal control problems in the presence of gravitational forces [19]. When a movement consists of a transition between two equilibrium postures, the boundary conditions of the optimal control problem should specify terminal equilibrium signals, e.g. muscle forces which compensate for applied static (elastic, gravitational) forces. The idea to add to the cost function a term which enforces given initial and final equilibrium postures should lead to solutions which depend on the level and nature of the static forces [17]. In contrast, the previously introduced separation principle provides a way to apply optimal feedback control to kinematic redundancy problems with static forces, as there is no a priori specification of the final posture of the limb.

Maximum efficiency: The energy of the signals of motoneurons, that eventually generate the dynamic forces, is continuously minimized along the motion. The system attempts to reach the goal with zero error and minimal control signals. Note that, compared to other cost functions encountered in the motor control literature (jerk [15], torque change [16], variance [17], energy [20], etc.) this cost function is easily measurable by the CNS. Furthermore, the constraint functions used in this model are the initial and final boundary conditions that lead to an univocal description of motor control, contrary to models involving related cost function such as error/effort minimization [18].

Constant effort principle : The idea of motor behavior being associated with the minimum of a cost function is appropriate when both movement amplitude and duration are specified. Otherwise, infinitely slow/fast or infinitely short/long movements could result. The constant effort principle states that a given set of instruction is equivalent to a level of effort. For these instructions, movements of different amplitudes, directions, or against different loads are executed with the same effort.

III. MODEL AND PROBLEM STATEMENT

The separation principle stated in the preceding section can be easily applied to the control design of robots such as HRP2, in which each joint is independently regulated to a reference angular value. Indeed, the robustness of the low-level control of each link allows to make the hypothesis that static forces are exactly counterbalanced. The synthesis of a controller can then be obtained by disregarding static effects. In this way, the optimization problem can be solved on the basis of a simplified model describing the phasic component only. In order to implement this model on the robot, we developed a global model that contains the dynamics of the $n = 6$ DOF arm and includes, for each degree of freedom, the dynamics of the neuromuscular system associated to a pair of virtual antagonist muscles. In this way, the considered system input are the neural control signals of the virtual motoneurons. Each muscle i ($1 \leq i \leq 2n$) is controlled by a motoneuron and, according to [21], the set motoneuron + muscle (neuromuscular system) can be described by a second-order low-pass filter having the neural control signal u_i as input and the muscular force F_i as output, according to the following scheme

$$\begin{aligned} v(de_i/dt) &= -e_i + u_i \\ v(da_i/dt) &= -a_i + e_i \\ F_i &= \eta(a_i) \end{aligned} \quad (1)$$

where v is a time constant. The function η (used to express the fact that a muscle exerts a pulling force only) is defined by $\eta(z) = z$ if $z > 0$; otherwise, $\eta(z) = 0$. The variables e_i and a_i correspond to excitation and activation parameters¹. As $\eta(z)$ is not differentiable at the origin, it can be replaced by the function $z \rightarrow \log[1.0 + \exp(\kappa z)]/\kappa$, with $\kappa > 0$. Torques τ_k were calculated at each DOF from the difference between the forces generated by antagonist muscles scaled by a coefficient γ_k (in meters), as described in (2).

$$\tau_k = \gamma_k(F_{2k-1} - F_{2k}), \quad k = 1 \dots n. \quad (2)$$

The robotics arm of HRP2 (see figure 1) has six DOF: three at the shoulder, two at the elbow and one at the hand (see [22] for details), the grasping DOF of the hand being not considered here. We used the Lagrangian approach to express the equation of dynamics of this rigid, multi-linked, articulated system [23]. The computation was done through the symbolic calculus tools in Matlab. On this basis, the equivalent C code was generated for the optimization program described § IV. The arm dynamics can be expressed under the usual form

$$\tau = M(q)\ddot{q} + N(q, \dot{q})\dot{q} + G(q) \quad (3)$$

where M is the inertia matrix, N is a nonlinear vector including Coriolis effects, G is a vector related to gravity efforts, τ is the torque vector that generates the movement, q , \dot{q} , \ddot{q} are the vectors of angular position, velocity and

¹The Electromyographic activity (EMG) usually corresponds to $\eta(e_i)$

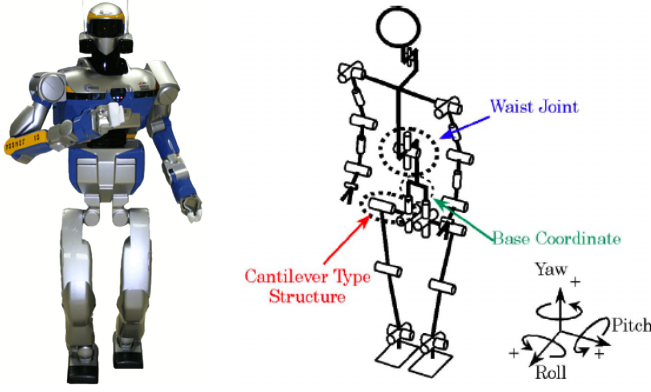


Fig. 1. Humanoid robot HRP2 and its mechanical structure.

acceleration of successive links. According to the separation principle, for the computation of optimal trajectories, the term $G(q)$ which correspond to static efforts can be removed from (3). So, the relationship between angular accelerations and torques can be expressed as follows

$$\ddot{q} = M^{-1}(\tau - N\dot{q}) \quad (4)$$

By gathering the arm dynamics described by (4) with the actuation dynamics associated to each of the six pairs of virtual muscles described by (1) we obtained a 36 dimensional dynamical system of the form

$$\dot{x} = f(x(t), u(t)) \quad (5)$$

whose state is defined by

$$\begin{aligned} x^T &= (x_1, \dots, x_{36}) \\ &= (q_1, \dots, q_6, \dot{q}_1, \dots, \dot{q}_6, a_1, \dots, a_{12}, e_1, \dots, e_{12}) \end{aligned}$$

where q_1, \dots, q_6 are the angular coordinates, $\dot{q}_1, \dots, \dot{q}_6$ are the angular velocities, and for $i = 1, \dots, n$, (a_{2i-1}, a_{2i}) and (e_{2i-1}, e_{2i}) represent the activation and excitation parameters respectively, associated to the pair of antagonist muscles corresponding to the i^{th} DOF. The control vector, $u^T = (u_1, \dots, u_{12})$ is of dimension $n \times 2 = 12$. For $i = 1, \dots, n$, (u_{2i-1}, u_{2i}) represent the motoneurons signals associated to the pair of antagonist muscles corresponding to the i^{th} DOF. Note that the derivatives of the state variables x_i are computed as follows: for $i = 1, \dots, 6$, $\dot{x}_i = \dot{q}_i = x_{i+6}$, for $i = 7, \dots, 12$, \dot{x}_i are given by (4) and for $i = 13, \dots, 36$, \dot{x}_i are deduced from (1).

Given a current arm configuration x_0 at time t_0 and a target position of the hand at time t_f , and according to the optimal feedback control principle and the maximum efficiency principle, the trajectory of the global system must minimize the energy of motoneurons along the time interval $[t_0, t_f]$. This problem can be stated as an optimal control problem as follows: find a deterministic control $u(t) = \{u_i(t)\}$ ($1 \leq i \leq 2n$) over $[t_0, t_f]$ such that $x(t)$ is a solution of (5) satisfying the following boundary conditions

$$x(t_0) = x_0 \quad \text{and} \quad \psi(x(t_f)) = 0, \quad (6)$$

while minimizing the quantity

$$E = \sum_{i=1}^{2n} \int_{t_0}^{t_f} u_i^2(t) dt \quad (7)$$

In relation (6), $\psi(x(t_f))$ expresses the constraint on the state at time t_f , which corresponds to the specified final hand position at which $\dot{q}(t_f) = a(t_f) = e(t_f) = 0$. As explained in the next section, this final condition can be deduced from the expression of the direct kinematics at time t_f . Considering that the robot arm is at rest at t_0 , the initial condition is given by

$$x_0^T = (q_1^0, \dots, q_6^0, 0, \dots, 0) \quad (8)$$

where q_1^0, \dots, q_6^0 are the initial angular values of the robot joints at t_0 .

IV. OPTIMIZATION

To solve the two-point boundary-value problem stated by (5), (6), (7) we used a direct transcription method [24]. Following this approach, the original problem can be transformed into a discretized version which then can be solved by a large-sparse NonLinear Programming (NLP) method, such as the interior point method implemented in the Ipopt software [25]. The main steps of the method are presented in the sequel, more details can be found in [24].

A. Direct Transcription

The first step of the direct transcription approach is to determine the vector of variables of the corresponding NLP problem. It consists in discretizing the time interval of movement duration $[t_0, t_f]$ into $m + 1$ time-points as follows

$$t_0 = t_0 < t_1 < t_2 < \dots < t_m = t_f \quad (9)$$

At each time-point, the state vector and the control vector are both specified. As a consequence, the discretized version of the variable vector has the form

$$\begin{aligned} \chi^T &= (x_1^0, \dots, x_{36}^0, u_1^0, \dots, u_{12}^0, \\ &\quad x_1^1, \dots, x_{36}^1, u_1^1, \dots, u_{12}^1, \\ &\quad \dots, \\ &\quad x_1^m, \dots, x_{36}^m, u_1^m, \dots, u_{12}^m) \end{aligned} \quad (10)$$

where x_i^k and u_i^k correspond to system states and controls at t_k . This vector χ includes $l = (m + 1) \times (36 + 12)$ variables.

The next step is to represent the constraints. Here we have two types of constraint, one on the dynamics (5) and another one on the ψ function (6). The description of variables in (10) conducts to the following trapezoidal representation of dynamical constraints

$$\begin{aligned} x_i^{k+1} - x_i^k - \frac{h_k}{2}(f_i^k + f_i^{k+1}) &= 0 \\ i &= 1 \dots 36, \quad k = 0 \dots m - 1 \end{aligned} \quad (11)$$

where $h_k = t_{k+1} - t_k$ is the duration of the time interval $[t_k, t_{k+1}]$. So, the number of dynamical constraints is equal to $d = m \times 36$. The condition $\psi(x(t_f)) = 0$, which expresses the fact that the hand must reach the target at the final time t_f , is defined by the following equations

$$|g(x_1^m, x_2^m, x_3^m, x_4^m, x_5^m, x_6^m) - P_t| = 0 \quad (12)$$

$$x_7^m = x_8^m = \dots = x_{36}^m = 0 \quad (13)$$

where g is the direct kinematics function which calculates the position of the hand in Cartesian coordinates from the angular value of each link, and P_t is the desired target point. The constraints corresponding to the initial boundary conditions (8) are represented by

$$\begin{cases} \text{for } i = 1..6, & x_i^0 = q_i^0 \\ \text{for } i = 7..36, & x_i^0 = 0 \end{cases} \quad (14)$$

One important advantage of the direct transcription method is that additional constraints can be easily taken into account by introducing bounds on the state variables. For the case of the HRP2 arm, the angular constraints are as follows

$$\text{for } i = 1..6, \quad x_i^{min} < x_i^0, x_i^1, \dots, x_i^m < x_i^{max} \quad (15)$$

Finally, the cost to minimize in (7) can be expressed as a finite sum computed at all discretized time points

$$E(\chi) = \sum_{i=1}^{2n} \sum_{k=0}^m (u_i^k)^2 \quad (16)$$

B. NLP Solving

By (10)–(16) we have formulated a large-sparse NLP problem from an optimal control problem, which has the form

$$\begin{aligned} & \min_{\chi \in \mathbb{R}^l} E(\chi) \\ & \text{such that : } \quad c_L \leq c(\chi) \leq c_U \\ & \quad \quad \quad \chi_L \leq \chi \leq \chi_U \end{aligned} \quad (17)$$

where $E(\chi) : \mathbb{R}^l \rightarrow \mathbb{R}^+$ is the objective function, and $c(\chi) : \mathbb{R}^l \rightarrow \mathbb{R}^d$ are the constraint functions. The vectors c_L and c_U denote the lower and upper bounds on the constraints, and the vectors χ_L and χ_U are the bounds on the variables χ . For the considered problem, the vector χ is defined by (10), $E(\chi)$ is given by (16), $c(\chi)$ correspond to the functions in (11) and (12), where $c_L = c_U \equiv 0$, and the constraints on χ are represented by (13) and (14).

To solve the NLP problem, we used the Ipopt solver [25], which turned out to be efficient in terms of accuracy and convergence time. In practice, for the direct transcription, we took $m = 50$ or 100 for movements of 1 second and $m = 100$ or 200 for movements of 2 seconds, that correspond to 2448, 4848 and 9648 variables respectively.

V. SIMULATION

In order to generate a movement, the algorithm requires as input the initial angular configuration of the arm, the movement duration, and the position of the desired target expressed in a system of spherical coordinates (r, θ, ϕ) centered at the initial hand position. In this definition, r is the movement amplitude, θ and ϕ are the azimuth and elevation angles respectively. This representation is well appropriate for the description of movements starting with the same initial arm configuration and directed toward peripheral hand target positions.

The muscle parameters provided to the system were chosen in the same way as in [9]: $v = 0.05s$ (time constant of muscle filtering), and $\kappa = 10$ (force generation characteristics of the muscle). Moreover, as stated by (2) at each DOF, the link between the force generated by the pair of muscles and the torque is related to a coefficient γ_k . The choice of these coefficients is somewhat arbitrary and discussed in [9]. In our program, we did not try to find the best values of γ_k for all movements. The durations of movements were adapted to the robot dynamics, they were a little bit increased with respect to durations in [9].

Figures 2 and 3 represent the shape of trajectories of amplitude 25cm and duration 1 second, ending at twenty evenly spaced peripheral hand positions in the frontal and sagittal plane respectively. These target positions correspond to nonsingular configurations of the robot. The initial configuration of the robot arm is $(5^\circ, -15^\circ, 30^\circ, -110^\circ, 0^\circ, 0^\circ)$.

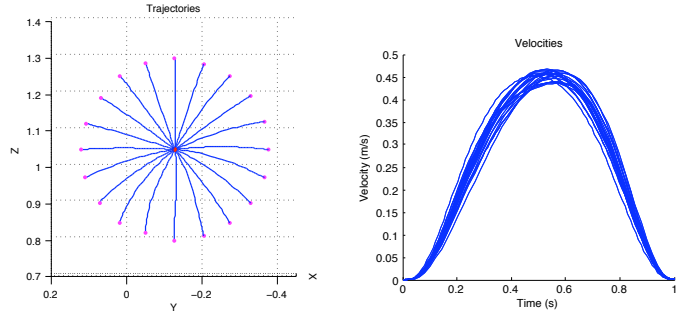


Fig. 2. Movements of amplitude $r = 25cm$, starting with the same arm configuration, and ending at twenty evenly spaced peripheral targets in the frontal plane.

Figure 4 shows in detail the variation of motion parameters during a simulated movement of the hand of amplitude $r = 25cm$ to the direction $(\theta, \phi) = (-45^\circ, 45^\circ)$.

As a result, it is interesting to remark that the robot trajectories obtained through this approach exhibit the principal characteristics of human motions, as reported in [9] and [26]. Indeed, the hand trajectories are almost rectilinear and the corresponding velocity profiles are single-peak and bell-shaped. Figure 5 shows two sets of human hand paths

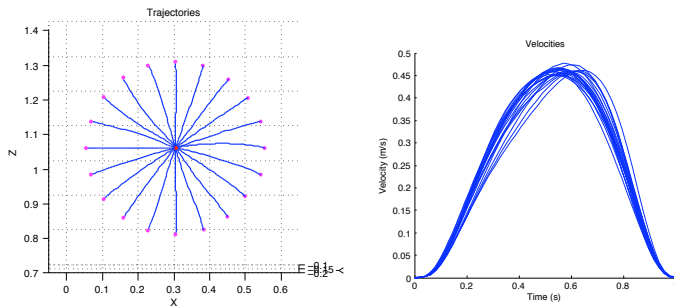


Fig. 3. Movements of amplitude $r = 25\text{cm}$, starting with the same arm configuration, and ending at twenty evenly spaced peripheral targets in the sagittal plane.

starting with the same arm configuration and ending at peripheral targets locations in the sagittal and the frontal plane respectively. These trajectories look very similar to the ones executed by HRP2, which are represented in figures 2 and 3. Furthermore, the slight curvature variation associated to the circular distribution of targets seems to obey the same rule in both cases. Concerning the accuracy of our result, the average difference between the final robot hand position and the target is very small, around 1 mm, and the average of maximum distance to a virtual reference straight line trajectory is about 1 cm.

In order to demonstrate that the control approach is not limited to short motions, the method has also been tested for movements of amplitude 50 cm with duration of 2 seconds. Single peak bell-shaped velocity curves still occur, though the trajectory is unsurprisingly more curved (the average distance to the straight line is about 4 cm). The target-hand distance error at final time is still small, about 1 mm. Figure 6 shows two examples of such motions obtained with the simulation software OpenHRP and figure 7 shows corresponding hand trajectories and velocities. To simulate motions with OpenHRP, we took the angular trajectory of the robot joints obtained from the optimization program and then interpolated it to determine the input data. The simulator then follows the input data to display the movement by taking into account the exact parameters of the robot. Such a validation on OpenHRP guarantees that the movement will be correctly executed by the real robot.

In our simulations, a movement generation normally takes from 1 to 4 minutes depending on the amplitude of the motion and the choice of parameters. The program Ipopt converged to satisfy the constraints with very good accuracy after around 200 to 300 iterations but it did not always finish properly. This may be due to numerical errors in dynamics calculations or to the approximation of the Hessian in the program. This phenomenon was also pointed out in [27]. Finally, the performance of the program could be improved by completing the refinement step in the direct transcription approach. Videos showing different motions are available at <http://www.laas.fr/~tmtuan/works/>

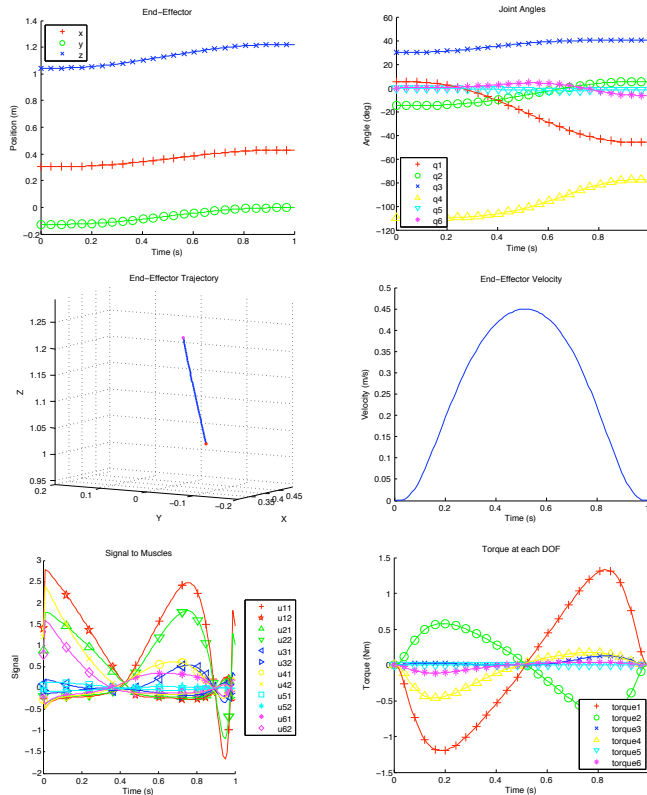


Fig. 4. Evolution of motion parameters during a movement of amplitude $r = 25\text{cm}$ to the direction $(\theta, \phi) = (-45^\circ, 45^\circ)$. Left up: Cartesian coordinates of the hand; right up: angular trajectory; left middle: hand trajectory; right middle: hand velocity; left down: control signals; right down: torques.

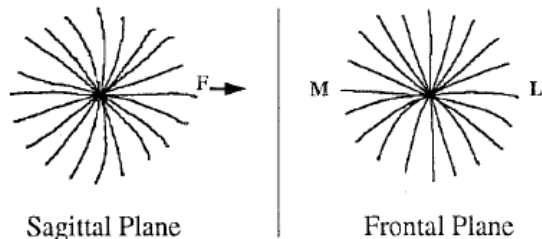


Fig. 5. Human reaching hand paths as reported by Flanders et al. in [26]. The situation is similar to the one described in figures 2 and 3: targets are arranged at twenty peripheral positions located at 30cm from the initial hand location. F, M and L stand for forward, right and left respectively.

VI. CONCLUSION

The interest of applying neurobiological principle to the control of humanoid robots has been illustrated in the case of reaching motions. Beyond the capacity of producing realistic movements, the proposed approach has two main interest from the control point of view. First, the separation of dynamic and static efforts allows to simplify the optimization problem which leads to the characterization of trajectories. The hypothesis that static gravitational efforts are continuously compensated by the tonic control is particularly well

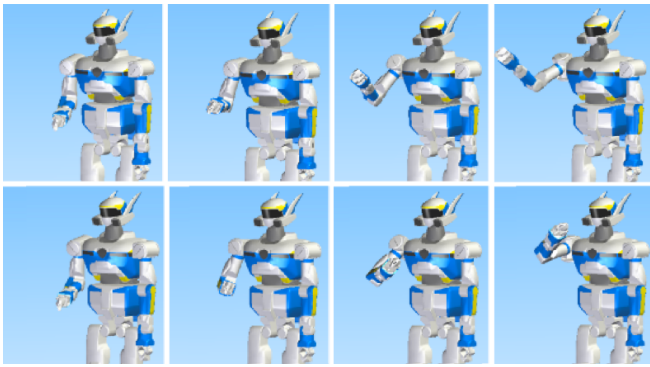


Fig. 6. Two movements of amplitude $r = 50\text{cm}$ simulated with OpenHRP. Each movement is illustrated by four successive views arranged from left to right. The first movement (top line) is directed to $(-35^\circ, 35^\circ)$ whereas the second one (bottom line) is directed to $(40^\circ, 25^\circ)$.

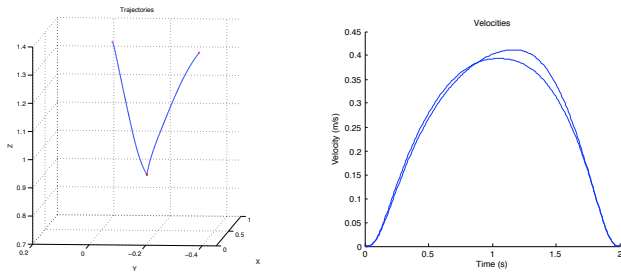


Fig. 7. Hand trajectories (left image) and velocities (right image) corresponding to the two reaching movements represented in figure 6.

grounded in the case of robotic systems such as the humanoid HRP2, for which each link is individually regulated to a reference value. Second, as the solution of an inverse kinematics problem is not required, the redundancy problem can be solved at low computational cost for a six DOF arm. Thanks to the direct transcription method and the Ipopt software which give performance and flexibility to our optimization program, further constraints such as the bounds on articular joints, the Zero-Moment Point (ZMP), or obstacles avoidance can be easily added in the program. On this basis, we are currently working on an extension of the approach to control whole body reach-to-grasp movements.

VII. ACKNOWLEDGMENT

This work was partially supported by the Zeuxis project funded by the EADS foundation and by the ROMA project financed by the CNRS within the framework of the interdisciplinary programme NeuroInformatique.

REFERENCES

- [1] K. Tahara, Z. Luo, and S. Arimoto. On control mechanism of human-like reaching movements with musculo-skeletal redundancy. In *IEEE/RSJ Int. Conf. on Intelligent Robots and Systems*, 2006.
- [2] S. Northrup, N. Sarkar, and K. Kawamura. Biologically-inspired control architecture for a humanoid robot. In *In: Proc IEEE/RSJ Int. Conf. on Intelligent Robots and Systems, Vol 2, pp 1100-1105*, 2001.
- [3] G. Simmons and Y. Demiris. Optimal robot arm control using the minimum variance model. *J Robot Syst*, 22(11):677–690, 2005.
- [4] T. Matsui, M. Honda, and N. Nakazawa. A new optimal control model for reproducing human arm's two-point reaching movements: A modified minimum torque change model. In *Proc IEEE International Conference on Robotics and Biomimetics*, pp 1541-1546, 2006.
- [5] H. Seki and S. Tadakuma. Minimum jerk control of power assisting robot based on human arm behavior characteristics. In *Proc IEEE Int.Conf. on Syst, Man and Cybernetics, Vol 1, pp 722-727*, 2004.
- [6] M. Hersch and Billard A.G. A biologically-inspired controller for reaching movements. *IEEE/RAS-EMBS International Conference on Biomedical Robotics and Biomechatronics*, 2006.
- [7] Mataric M. Getting humanoids to move and imitate. In *IEEE Intelligent Systems*, 2000.
- [8] Y. Fujita, Y. Nakamura, K. Yamane, and Suzuki I. Somatosensory computation for man-machine interface from motion-capture data and musculoskeletal human model. *IEEE Trans. On Robotics* 21(1):58-66, 2004.
- [9] E. Guigon, P. Baraduc, and M. Desmurget. Computational motor control: Redundancy and invariance. *J Neurophysiol*, 97(1):331–347, 2007.
- [10] E. Guigon, P. Baraduc, and M. Desmurget. Optimality, stochasticity, and variability in motor behavior. *J Comput Neurosci*, 24(1):57–68, 2008.
- [11] M.K. Rand, Y. Shimansky, G.E. Stelmach, and J.R. Bloedel. Adaptation of reach-to-grasp movement in response to force perturbations. *Exp Brain Res*, 154: 50-65, 2004.
- [12] T.G. Welter and M.F. Bobbert. Initial muscle activity in planar ballistic arm movements with varying external force directions. *Motor Control*, 6: 32-51, 2002.
- [13] J.F. Kalaska, Cohen D.A.D., M.L. Hyde, and M. Prud'homme. A comparison of movement direction-related versus load direction-related activity in primate motor cortex, using a two-dimensional reaching task. *J Neurosci*, 9: 2080-2102, 1989.
- [14] K.C. Nishikawa, S.T. Murray, and M. Flanders. Do arm postures vary with the speed of reaching. *J Neurophysiol*, 81: 2582-2586, 1999.
- [15] T. Flash and N. Hogan. The coordination of arm movements: An experimentally confirmed mathematical model. *J Neurosci*, 5: 1688-1703, 1985.
- [16] Y. Uno, M. Kawato, and R. Suzuki. Formation and control of optimal trajectory in human multijoint arm movement - minimum torque change model. *Biol Cybern*, 61(2):89–101, 1989.
- [17] C.M. Harris and D.M. Wolpert. Signal-dependent noise determines motor planning. *Nature*, 394(6695):780–784, 1998.
- [18] E. Todorov and M.I. Jordan. Optimal feedback control as a theory of motor coordination. *Nat Neurosci*, 5(11):1226–1235, 2002.
- [19] K.A. Thoroughman and K.J. Feller. Gravitational effects on torque change and variance optimization in reaching movements program no. 492.20. abstract viewer/itinerary planner. *Washington, DC: Society for Neuroscience, Online*, 2003.
- [20] R.M. Alexander. Optimization and gaits in the locomotion of vertebrates. *Physiol Rev*, 69(4):1199–1227, 1989.
- [21] F.C.T. Van der Helm and L.A. Rozendaal. Musculoskeletal systems with intrinsic and proprioceptive feedback. *Neural control of posture and movement*, 2000.
- [22] K. Kaneko, F. Kanehiro, S. Kajita, H. Hirukawa, T. Kawasaki, M. Hirata, K. Akachi, and T. Isozumi. Humanoid robot hrp-2. *ICRA IEEE*, 2004.
- [23] M.S. Spong and M. Vidyasagar. *Robot Dynamics and Control*. Wiley, 1989.
- [24] J.T. Betts. *Practical Methods for Optimal Control Using Nonlinear Programming*. Society for Industrial Mathematics, 2001.
- [25] A. Wächter and L.T. Biegler. On the implementation of a primal-dual interior point filter line search algorithm for large-scale nonlinear programming. *Mathematical Programming* 106(1), pp. 25-57, 2006.
- [26] M. Flanders, J.J. Pellegrini, and S.D. Geisler. Basic features of phasic activation for reaching in vertical planes. *Exp Brain Res*, 1996.
- [27] S. Miossec, S. Yokoi, and K. Kheddar. Development of a software for motion optimization of robots - application to the kick motion of the hrp-2 robot. *ICRA IEEE*, 2006.